Paramagnetic Anisotropy and Electronic Structure of [*NN'*-Ethylenebis(salicylideneiminato)]cobalt(II), its Pyridine Adduct, and [*NN'*-Ethylenebis(thiosalicylideneiminato)]cobalt(II)

By **Keith S. Murray** * and **Robert M. Sheahan**, Chemistry Department, Monash University, Clayton, Victoria 3168, Australia

Single-crystal magnetic-anisotropy measurements have been made over the temperature range 80—300 K on the oxygen-inactive title chelates [{Co(salen)}$_2$], [Co(salen)]·py, and [{Co(tsalen)}$_2$]. These five-co-ordinate species all show rhombic magnetic ellipsoids with [{Co(tsalen)}$_2$] being the least anisotropic. Both salen complexes display an unusually rapid increase in magnetic moment at higher temperatures. The theoretical model developed to interpret the results incorporates spin–orbit coupling between the ground doublet state and the excited doublet and quartet states, the latter being low-lying and important in the case of the salen complexes. Small changes in ligand field with temperature have been invoked to explain the rapid increases in μ_i at higher temperatures. The relative ordering of the cobalt *d*-orbital levels has been deduced, and correlations between the positions of the out-of-plane π orbitals, d_{xz} and d_{yz}, and the bonding of the axial donor ligands (*e.g.* pyridine) and of O$_2$ are briefly discussed.

SINCE the early work of Tsumaki,[1] and Calvin[2] and their co-workers, there has been continued interest in the properties of low-spin cobalt(II) Schiff-base chelate complexes. This is chiefly due to the unusual reactivity displayed by this important class of compounds. The complexes are best known for their ability, under certain conditions, to reversibly co-ordinate oxygen both in the crystalline state and in solution, and this has led to their use as models for biological oxygen carriers[3-6] and to their application as catalysts for certain organic oxidations.[4,7] They also form very stable cobalt–carbon σ-bonded organometallic compounds which have served as important model systems for vitamin B$_{12}$ coenzyme.[8]

It seemed to us important, therefore, to obtain a detailed picture of the electronic structures of such complexes and to this end we have investigated the anisotropy in the magnetic susceptibility of single crystals of a range of salicylaldimine and acetylacetoneimine derivatives. The theoretical analysis of the principal susceptibility measurements, obtained over a wide temperature range, has yielded the relative ordering of the *d*-orbital energy levels. We discuss here the results obtained for three examples of the salicylaldimine type, [{Co(salen)}$_2$], [Co(salen)]·py, and [{Co(tsalen)}$_2$],† all of which are inactive towards oxygen in the crystalline state, but active to varying extents in solution. Average susceptibility measurements on polycrystalline samples of [{Co(salen)}$_2$] and [Co(salen)]·py have been made previously.[9] Recently there have been numerous e.s.r. studies on complexes of this type in powder form or in frozen solvents, which have yielded some information on the ground state and orbital occupancy.[10-17] Some

---

† salen = *NN'*-Ethylenebis(salicylideneiminato), tsalen = *NN'*-ethylenebis(thiosalicylideneiminato), and py = pyridine.

[1] T. Tsumaki, *Bull. Chem. Soc. Japan*, 1938, **13**, 252.

[2] A. E. Martell and M. Calvin, 'Chemistry of Metal Chelate Compounds,' Prentice Hall, New York, 1952.

[3] E. Bayer and P. Schretzmann, *Structure and Bonding*, 1967, **2**, 181.

[4] G. Henrici-Olive and S. Olive, *Angew. Chem. Internat. Edn.*, 1974, **13**, 1.

[5] A. L. Crumbliss and F. Basolo, *J. Amer. Chem. Soc.*, 1970, **92**, 55.

[6] G. A. Rodley and W. T. Robinson, *Nature*, 1972, **235**, 438.

[7] M. Fieser and L. F. Fieser, 'Reagents for Organic Synthesis,' Wiley, 1972, vol. 3, p. 245.

[8] D. Dodd and M. D. Johnson, *J. Organometallic Chem.*, 1973, **52**, 1.

[9] A. Earnshaw, P. C. Hewlett, E. A. King, and L. F. Larkworthy, *J. Chem. Soc.* (*A*), 1968, 241.

[10] B. M. Hoffman, D. L. Diemente, and F. Basolo, *J. Amer. Chem. Soc.*, 1970, **92**, 61.

[11] C. Busetto, F. Cariati, A. Fusi, M. Gullotti, F. Morazzoni, A. Pasini, R. Ugo, and V. Valenti, *J.C.S. Dalton*, 1973, 754.

[12] C. Busetto, F. Cariati, P. Fantucci, D. Galizzioli, and F. Morazonni, *J.C.S. Dalton*, 1973, 1712.

[13] E. I. Ochiai, *J. Inorg. Nuclear Chem.*, 1973, **35**, 1727.

[14] Y. Nishida and S. Kida, *Bull. Chem. Soc. Japan*, 1972, **45**, 461.

[15] A. von Zelewsky and H. Fierz, *Helv. Chim. Acta*, 1973, **56**, 977.

[16] L. M. Engelhardt, J. D. Duncan, and M. Green, *Inorg. Nuclear Chem. Letters*, 1972, **8**, 725.

[17] R. Karlsson, L. M. Engelhardt, and M. Green, *J.C.S. Dalton*, 1972, 2463.

of our results have been presented in a preliminary communication.[18]

EXPERIMENTAL

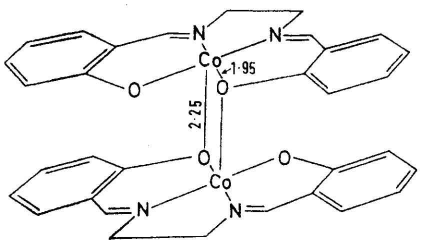

(I)

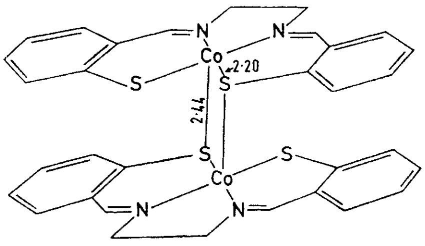

(II)

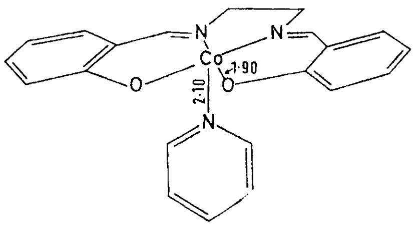

(III)

Large crystals of [{Co(salen)}$_2$] and [Co(salen)]·py were grown as described previously;[18] [{Co(tsalen)}$_2$] was synthesized as described [19] and crystals were grown from *NN*-dimethylformamide (dmf) solution using the same sealed-tube techniques as for the other crystals. The crystals of [{Co(tsalen)}$_2$] were much smaller than the others, *ca.* 0.2 mg, but were sufficiently large to obtain reproducible anisotropy data.

The anisotropy measurements over the temperature range 90—300 K were made using a null-deflection torsion balance, described earlier. The wheel device of Gerloch and Quested was employed for the monoclinic crystals of [{Co(salen)}$_2$].[20] The smaller crystals of [{Co(tsalen)}$_2$] were mounted along the a^*, b, and c axes respectively. Crystal axes were located by *X*-ray photography. Powder susceptibilities were determined by the Gouy method in the liquid-nitrogen range, and on a Foner vibrating-sample magnetometer in the range 4—77 K for [{Co(salen)}$_2$].

Crystal Structures.—The complexes [{Co(salen)}$_2$] and [{Co(tsalen)}$_2$] are both monoclinic, with four centrosymmetric dimer groups in the unit cell.[21-23] They have similar molecular structures, (I) and (II), in which ligand-bridged dimerization occurs to give square-pyramidal stereochemistry around each cobalt. The complex [Co(salen)]·py is orthorhombic and has a monomeric square-pyramidal structure, (III), in which the plane of the pyridine ring bisects the ligand N,O direction.[24]

RESULTS

The crystal anisotropies, χ_i, and average susceptibilities, $\bar{\chi}$, over the range 90—300 K are given in Table 1. The principal molecular susceptibilities, K_i, were obtained from these by the tensor-transformation methods of Krishnan and Lonsdale.[25] For the monoclinic crystals of [{Co(salen)}$_2$] and [{Co(tsalen)}$_2$] the modified approach of Gerloch and Quested was employed to obtain the best set of direction cosines.[20] Assumption of rhombic symmetry gave an excellent fit at all temperatures. The direction cosines for these and orthorhombic [Co(salen)]·py are given in Table 2. The derived molecular-susceptibility ellipsoids for the

TABLE 1

Experimental† crystal anisotropies and average susceptibilities (10^6 cm^3 mol^{-1})

(*a*) [{Co(salen)}$_2$]

T/K	*b* axis (χ_3) vertical ($\chi_2 - \chi_1$)	χ_2 vertical ($\chi_3 - \chi_1$)	$\bar{\chi}$
320	408	1 140	1 943
300	392	1 145	1 952
280	383	1 160	1 996
260	384	1 198	2 082
240	394	1 258	2 193
220	410	1 333	2 320
200	432	1 419	2 471
180	462	1 529	2 660
160	495	1 665	2 882
140	538	1 833	3 167
120	595	2 090	3 549
100	670	2 418	4 032

(*b*) [Co(salen)]·py

	a axis vertical ($\chi_c - \chi_b$)	*c* axis vertical ($\chi_a - \chi_b$)	
320	775	476	2 279
300	725	423	2 200
280	687	380	2 178
260	664	350	2 194
240	655	335	2 260
220	666	320	2 376
200	692	330	2 536
180	735	343	2 735
160	797	371	2 985
140	884	412	3 300
120	999	466	3 710
100	1 166	536	4 245

(*c*) [{Co(tsalen)}$_2$]

	b axis (χ_3) vertical ($\chi_2 - \chi_1$)	*c* axis vertical ($\chi_a{}^* - \chi$	a* axis vertical $\chi_c - \chi_3$)	$\bar{\chi}$
300	75	100	150	1 550
280	70	100	148	1 675
260	67	100	144	1 695
240	62	100	139	1 780
220	60	100	134	1 870
200	60	100	127	1 975
180	60	97	127	2 115
160	60	96	127	2 300
140	58	96	125	2 530
120	58	94	125	2 865
100	58	94	125	3 300

† The quoted values are smoothed data obtained for several crystals of each complex.

---

[18] K. S. Murray and R. M. Sheahan, *Chem. Phys. Letters*, 1973, **22**, 406.

[19] A. van den Bergen, M. F. Corrigan, K. S. Murray, R. M. Slade, and B. O. West, *Inorg. Nuclear Chem. Letters*, 1974, **10**, 859.

[20] M. Gerloch and P. N. Quested, *J. Chem. Soc.* (*A*), 1971, 2307.

[21] S. Brückner, M. Calligaris, G. Nardin, and L. Randaccio, *Acta Cryst.*, 1969, **B25**, 1671.

[22] R. de Iasi, B. Post, and S. L. Holt, *Inorg. Chem.*, 1971, **10**, 1498.

[23] M. F. Corrigan, K. S. Murray, R. M. Sheahan, B. O. West, G. D. Fallon, and B. M. Gatehouse, *Inorg. Nuclear Chem. Letters*, 1975, **11**,625.

[24] M. Calligaris, D. Minichelli, G. Nardin, and L. Randaccio, *J. Chem. Soc.* (*A*), 1970, 2411.

[25] K. S. Krishnan and K. Lonsdale, *Proc. Roy. Soc.*, 1936, **A156**, 597.

TABLE 2

Direction cosines

	[{Co(salen)}$_2$]			[{Co(tsalen)}$_2$]			[Co(salen)]·py		
	a	*b*	*c**	*a*	*b*	*c**	*a*	*b*	*c*
K_x	−0.1303	−0.9571	0.2588	0.3752	0.4844	−0.7903	−0.9999	0.0016	0.0057
K_y	0.9896	−0.1414	−0.0257	−0.1062	0.8695	0.4825	−0.0059	−0.2678	−0.9635
K_z	−0.0615	−0.2577	−0.9656	−0.9208	0.0971	−0.3776	0	0.9635	−0.2678

TABLE 3

Observed and calculated molecular susceptibilities (10^6 cm^3 mol^{-1}) and magnetic moments (1 B.M. ≈ 9.27 × 10^{-24} A m^2)

(*a*) [{Co(salen)}$_2$]

T/K	320	300	280	260	240	220	200	180	160	140	120	100
K_x (obs.)	2 669	2 687	2 746	2 860	3 014	3 192	3 401	3 664	3 978	4 376	4 934	5 641
K_y	1 813	1 810	1 842	1 915	2 011	2 122	2 258	2 427	2 624	2 877	3 206	3 623
K_z	1 347	1 359	1 400	1 471	1 554	1 645	1 754	1 888	2 044	2 247	2 506	2 832
K_x (calc.)	2 678	2 701	2 728	2 864	2 965	3 162	3 395	3 673	4 012	4 433	4 966	5 659
K_y	1 808	1 798	1 853	1 921	1 999	2 119	2 261	2 431	2 638	2 894	3 220	3 642
K_z	1 349	1 396	1 452	1 523	1 607	1 699	1 809	1 906	2 099	2 297	2 548	2 874
μ_x (obs.)	2.61	2.54	2.48	2.44	2.41	2.37	2.33	2.30	2.26	2.21	2.18	2.12
μ_y	2.15	2.08	2.03	2.00	1.96	1.93	1.90	1.87	1.83	1.80	1.75	1.70
μ_z	1.86	1.81	1.77	1.75	1.73	1.70	1.68	1.65	1.62	1.59	1.55	1.51
$\bar{\mu}$	2.23	2.17	2.11	2.08	2.05	2.02	1.99	1.96	1.92	1.88	1.85	1.80
μ_x (calc.)	2.62	2.55	2.47	2.44	2.39	2.36	2.33	2.30	2.27	2.23	2.18	2.13
μ_y	2.15	2.08	2.04	2.00	1.96	1.93	1.90	1.87	1.84	1.80	1.76	1.71
μ_z	1.86	1.83	1.80	1.78	1.76	1.73	1.70	1.67	1.64	1.60	1.56	1.52
$\bar{\mu}$	2.23	2.17	2.12	2.09	2.05	2.02	2.00	1.97	1.93	1.90	1.85	1.80
Fit	(a)	(b)	(c)	(d)	(e)	(e)	(e)	(e)	(e)	(e)	(e)	(e)

Best-fit parameters: ζ = 500 cm^{-1}, J = −40 cm^{-1}.

	Δ/cm^{-1}			
	$^4T_1$		$^2T_2(^1E)$	
	x,y	z	ξ	η
(a)	1 500	1 000	2 300	10 000
(b)	2 000	1 300	10 000	2 500
(c)	4 000	1 400	3 000	12 000
(d)	4 000	1 500	3 000	12 000
(e)	4 000	1 500	3 300	14 000

$\Delta(^2T_1)(^3A_2)$ x = 2 000, y = 1 200, z = 6 000
$\Delta(^2T_1)(^1E)$ x = 2 000, y = 15 000, z = 20 000

(*b*) [Co(salen)]·py

T/K	320	300	280	260	240	220	200	180	160	140	120	100
K_x (obs)	2 702	2 603	2 567	2 575	2 640	2 769	2 945	3 172	3 459	3 826	4 304	4 941
K_y	2 338	2 241	2 203	2 206	2 265	2 368	2 526	2 719	2 967	3 281	2 688	4 214
K_z	2 797	1 757	1 765	1 800	1 875	1 991	2 137	2 314	2 529	2 794	3 138	3 580
K_x (calc.)	2 700	2 602	2 555	2 555	2 667	2 791	2 936	3 161	3 442	3 803	4 284	4 957
K_y	2 369	2 250	2 196	2 212	2 296	2 388	2 523	2 712	2 949	3 253	3 658	4 224
K_z	1 804	1 766	1 775	1 823	1 908	2 015	2 146	2 301	2 498	2 751	3 089	3 564
μ_x (obs.)	2.63	2.50	2.40	2.31	2.25	2.21	2.17	2.14	2.10	2.07	2.03	1.99
μ_y	2.45	2.32	2.22	2.14	2.09	2.04	2.01	1.98	1.95	1.92	1.88	1.84
μ_z	2.14	2.05	1.99	1.93	1.90	1.87	1.85	1.83	1.80	1.77	1.74	1.69
$\bar{\mu}$	2.42	3.30	2.21	2.14	2.08	2.04	2.01	1.98	1.95	1.92	1.89	1.84
μ_x (calc.)	2.63	2.50	2.39	2.31	2.26	2.22	2.17	2.13	2.10	2.06	2.03	1.99
μ_y	2.46	2.32	2.22	2.15	2.10	2.05	2.01	1.98	1.94	1.91	1.87	1.84
μ_z	2.15	2.06	1.99	1.95	1.91	1.88	1.85	1.82	1.79	1.76	1.72	1.69
$\bar{\mu}$	2.42	2.30	2.21	2.14	2.10	2.05	2.01	1.98	1.94	1.91	1.88	1.84
Fit	(a)	(b)	(c)	(d)	(e)	(f)	(g)	(g)	(g)	(g)	(g)	(g)

Best-fit parameters: ζ = 500 cm^{-1}

	Δ/cm^{-1}			
	$^4T_1$		$^2T_2(^1E)$	
	x,y	z	ξ	η
(a)	750	500	4 000	17 500
(b)	900	750	4 200	17 500
(c)	1 100	1 000	4 500	17 500
(d)	1 500	1 300	5 000	17 500
(e)	1 800	1 500	5 000	17 500
(f)	2 000	1 800	5 000	17 500
(g)	2 000	2 000	5 200	17 500

$\Delta(^2T_1)(^3A_2)$ x,y = 750, z = 4 500
$\Delta(^2T_1)(^1E)$ x,y = 2 750, z = 8 750

TABLE 3 (*Continued*)

(*c*) [{Co(tsalen)}$_2$]

T/K	300	280	260	240	220	200	180	160	140	120	100
K_x (obs.)	1 702	1 773	1 839	1 919	2 005	2 108	2 247	2 431	2 659	2 994	3 428
K_y	1 555	1 632	1 703	1 790	1 880	1 984	2 123	2 308	2 538	2 873	3 308
K_z	1 393	1 470	1 542	1 631	1 724	1 833	1 975	2 160	2 392	2 728	3 163
K_x (calc.)	1 684	1 751	1 827	1 914	2 016	2 137	2 281	2 456	2 674	2 950	3 308
K_y	1 520	1 592	1 675	1 770	1 881	2 012	2 168	2 359	2 595	2 895	3 284
K_z	1 356	1 427	1 508	1 601	1 711	1 840	1 995	2 183	2 417	2 713	3 098
μ_x (obs.)	2.02	1.99	1.96	1.92	1.88	1.84	1.80	1.76	1.73	1.69	1.66
μ_y	1.93	1.91	1.88	1.85	1.82	1.78	1.75	1.72	1.69	1.66	1.63
μ_z	1.83	1.81	1.79	1.77	1.74	1.71	1.69	1.66	1.63	1.62	1.59
$\bar{\mu}$	1.93	1.91	1.88	1.85	1.81	1.78	1.75	1.72	1.69	1.66	1.62
μ_x (calc.)	2.01	1.98	1.95	1.92	1.88	1.85	1.81	1.77	1.73	1.68	1.63
μ_y	1.91	1.89	1.87	1.84	1.82	1.79	1.77	1.74	1.71	1.67	1.62
μ_z	1.80	1.79	1.77	1.75	1.74	1.72	1.69	1.67	1.65	1.61	1.57
$\bar{\mu}$	1.93	1.91	1.89	1.87	1.84	1.82	1.79	1.76	1.72	1.68	1.62

Best-fit parameters: $\zeta = 500$ cm^{-1}, $J = -40$ cm^{-1}, Δ in cm^{-1}.
$\Delta(^2T_2)(^1E)$ $\xi = 10\,000$, $\eta = 15\,000$. $\Delta(^2T_1)(^3A_2)$ $x = 1\,250$, $y = 2\,000$, $z = 12\,500$. $\Delta(^2T_1)(^1E)$ $x = 10\,000$, $y = 15\,000$, $z = 25\,000$

three complexes have K_x and K_y in the ligand plane and midway between the O,O (or S,S) and O,N (or S,N) donor atoms, respectively; K_z is at right angles to the plane, along the axial direction. In all cases $K_x > K_y > K_z$, with [{Co(tsalen)}$_2$] being less anisotropic than the other two complexes.

The K_i values (per cobalt atom) are given in Table 3. They have been given earlier [18] in graphical form where it can be seen that plots of $1/K_i$ against temperature for [{Co(salen)}$_2$] and [Co(salen)]·py exhibit maxima at *ca.* 300 and 270 K, respectively. In contrast, [{Co(tsalen)}$_2$] exhibits Curie–Weiss behaviour. The related plots of effective magnetic moment (per cobalt atom) showed a pronounced increase with temperature at higher temperatures for the salicylaldimine complexes, although not for the thiosalicylaldimine derivative (Figure 1). These increases were thought, at an early stage, to be indicative of excited quartet-state interactions. Measurements of $\bar{K}$ in the range 4—77 K were obtained for one of the complexes, [{Co(salen)}$_2$], and a susceptibility maximum was observed at *ca.* 46 K.

The Magnetic Model.—Low-spin d^7 cobalt(II) complexes have a ^2E ground state which is derived from the $t_2{}^6e^1$ orbital configuration (using octahedral notation for convenience). The theoretical model usually used to determine the magnetic and e.s.r. properties of such a system is that developed by Griffith [26] and (later) by Maki *et al.*[27] We have recently outlined the inadequacy of this simplified treatment,[28] which in essence considers the electronic states as single orbital wavefunctions, *i.e.* analogous to those of Cu^{II}, d^9. The present model, which is itself simplified to some extent, and which has many more additional parameters, does however lend itself to easy utility in the reproduction of principal magnetic moments and g values, something which could not always be obtained even qualitatively with the early model. It consists of the crystal-field–spin-orbit matrix $V_{\text{c.f.}} + \zeta\mathbf{l}.\mathbf{s}$, which uses states based on the electronic configurations $t_2{}^6e^1$ (ground) and $t_2{}^5e^2$ (excited). The states, which consist of various linear combinations of orbitals,[29] include spin doublets and quartets: ^2E; $^4T_1(^3A_2)$; $^2T_1(^3A_2)$; $^2T_1(^1E)$; $^2T_2(^1E)$; and $^2T_2(^1A_1)$. The strong-field limit was assumed with the parametrized crystal-field elements diagonal.

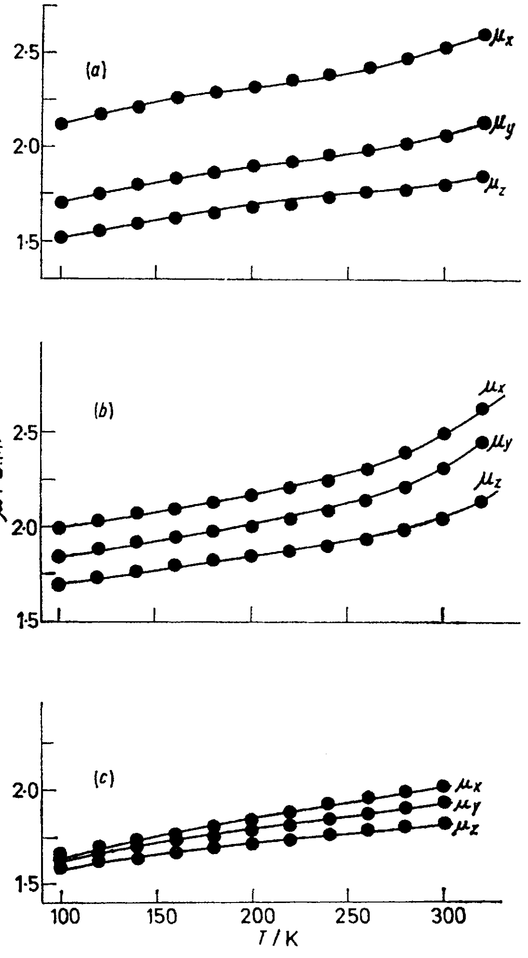

FIGURE 1 Temperature dependence of principal magnetic moments. Solid lines are calculated curves using parameters given in Table 3. (*a*), [{Co(salen)}$_2$]; (*b*) [Co(salen)]·py; (*c*), [{Co(tsalen)}$_2$]

Matrix elements between $^4T_1(^3A_2)$ and $^2T_1(^3A_2)$ were ignored. Further excited states arising from $t_2{}^4e^3$ and

---

[26] J. S. Griffith, *Discuss. Faraday Soc.*, 1958, **26**, 81.

[27] A. H. Maki, N. Edelstein, A. Davidson, and R. H. Holm, *J. Amer. Chem. Soc.*, 1964, **86**, 4580.

[28] K. S. Murray and R. M. Sheahan, *J.C.S. Chem. Comm.*, 1975, 475.

[29] J. S. Griffith, ' Theory of Transition Metal Ions,' Cambridge University Press, 1964.

$t_2^3e^4$ were excluded as these do not mix to first order by spin–orbit coupling with the ground state. Eigenvalues and eigenvectors were obtained on diagonalization of the matrix (see Table 4). The principal susceptibilities were then calculated in the usual way, using the Van Vleck equation; some pertinent aspects of the calculations are described below. No particular symmetry was assumed in the model, the energies of each excited state being parametrized relative to the ground state. The actual symmetry around the cobalt(II) atoms in the present chelates is C_s but is often approximated to C_{2v}.

TABLE 4

Off-diagonal non-zero matrix elements under spin–orbit coupling. Multiply each matrix element $A(a,b)$ by eζ, the spin–orbit coupling constant. $A(a,b) = A(b,a)$. The diagonal elements are the parametrized crystal-field energies

State number (a, b)	State *	
1	$^2E\ \frac{1}{2}\theta$	
2	$^2E - \frac{1}{2}\theta$	
3	$^4T_1\ \frac{3}{2}x\ (^3A_2)$	$A\ (3, 1) = -\frac{1}{2}$
4	$^4T_1\ \frac{1}{2}x\ (^3A_2)$	$A\ (4, 2) = -\ \frac{1}{2} \,.\, 3^{-\frac{1}{2}}$
5	$^4T_1 - \frac{1}{2}x\ (^3A_2)$	$A\ (5, 1) = \frac{1}{2} \,.\, 3^{-\frac{1}{2}}$
6	$^4T_1 - \frac{3}{2}x\ (^3A_2)$	$A\ (6, 2) = \frac{1}{2}$
7	$^4T_1\ \frac{3}{2}y\ (^3A_2)$	$A\ (7, 1) = -\frac{1}{2}, A\ (7, 3) = \frac{1}{2}$
8	$^4T_1\ \frac{1}{2}y\ (^3A_2)$	$A\ (8, 2) = -\frac{1}{2} \,.\, 3^{-\frac{1}{2}}, A\ (8, 4) = -\frac{1}{6}$
9	$^4T_1 - \frac{1}{2}y\ (^3A_2)$	$A\ (9, 1) = -\frac{1}{2} \,.\, 3^{-\frac{1}{2}}, A\ (9, 5) = -\frac{1}{6}$
10	$^4T_1 - \frac{3}{2}y\ (^3A_2)$	$A\ (10, 2) = A\ (10, 6) = -\frac{1}{2}$
11	$^4T_1\ \frac{1}{2}z\ (^3A_2)$	$A\ (11, 1) = -2 \,.\, 3^{-\frac{1}{2}}, A(11, 5) = -\frac{1}{3}, A(11, 3) = A\ (11, 7) = \frac{1}{2} \,.\, 3^{-\frac{1}{2}}$, ($A\ (11, 9) = \frac{1}{3}$
12	$^4T_1 - \frac{1}{2}z\ (^3A_2)$	$A\ (12, 2) = -2 \,.\, 3^{-\frac{1}{2}}, A\ (12, 6) = -\frac{1}{2} \,.\, 3^{-\frac{1}{2}}, A\ (12, 4) = A\ (12, 8) = \frac{1}{3}, A\ (12, 10) = \frac{1}{2} \,.\, 3^{-\frac{1}{2}}$
13	$^2T_1\ \frac{1}{2}x\ (^3A_2)$	$A\ (13, 2) = -\frac{1}{2} \,.\, 6^{-\frac{1}{2}}$
14	$^2T_1 - \frac{1}{2}x\ (^3A_2)$	$A\ (14, 1) = -\frac{1}{2} \,.\, 6^{-\frac{1}{2}}$
15	$^2T_1\ \frac{1}{2}y\ (^3A_2)$	$A\ (15, 2) = -\frac{1}{2} \,.\, 6^{-\frac{1}{2}}, A\ (15, 13) = \frac{1}{6}$
16	$^2T_1 - \frac{1}{2}y\ (^3A_2)$	$A\ (16, 1) = \frac{1}{2} \,.\, 6^{-\frac{1}{2}}, A(16, 14) = -\frac{1}{6}$
17	$^2T_1\ \frac{1}{2}z\ (^3A_2)$	$A\ (17, 1) = 6^{-\frac{1}{2}}, A\ (17, 14) = \frac{1}{6}, A\ (17, 16) = -\frac{1}{6}$
18	$^2T_1 - \frac{1}{2}z\ (^3A_2)$	$A\ (18, 2) = -6^{-\frac{1}{2}}, A\ (18, 13) = -\frac{1}{6}, A\ (18, 15) = -\frac{1}{6}$
19	$^2T_1\ \frac{1}{2}x\ (^1E)$	$A\ (19, 2) = \frac{1}{2} \,.\, 2^{-\frac{1}{2}}$
20	$^2T_1 - \frac{1}{2}x\ (^1E)$	$A\ (20, 1) = \frac{1}{2} \,.\, 2^{-\frac{1}{2}}$
21	$^2T_1\ \frac{1}{2}y\ (^1E)$	$A\ (21, 2) = \frac{1}{2} \,.\, 2^{-\frac{1}{2}}, A\ (21, 17) = -\frac{1}{4}$
22	$^2T_1 - \frac{1}{2}y\ (^1E)$	$A\ (22, 1) = -\frac{1}{2} \,.\, 2^{-\frac{1}{2}}, A\ (22, 18) = \frac{1}{4}$
23	$^2T_1\ \frac{1}{2}z\ (^1E)$	$A\ (23, 1) = -\frac{1}{2} \,.\, 2^{-\frac{1}{2}}, A\ (23, 18) = \frac{1}{4}, A\ (23, 20) = -\frac{1}{4}$
24	$^2T_1 - \frac{1}{2}z(^1E)$	$A\ (24, 2) = \frac{1}{2} \,.\, 2^{-\frac{1}{2}}, A\ (24, 19) = -\frac{1}{4}, A\ (24, 21) = -\frac{1}{4}$
25	$^2T_2\ \frac{1}{2}\xi\ (^1E)$	$A\ (25, 2) = \dfrac{3^{\frac{1}{2}}}{2.2^{\frac{1}{2}}}$
26	$^2T_2 - \frac{1}{2}\xi\ (^1E)$	$A\ (26, 1) = \dfrac{3^{\frac{1}{2}}}{2.2^{\frac{1}{2}}}$
27	$^2T_2\ \frac{1}{2}\eta\ (^1E)$	$A\ (27, 2) = \dfrac{-3^{\frac{1}{2}}}{2.2^{\frac{1}{2}}}, A\ (27, 25) = -\frac{1}{4}$
28	$^2T_2 - \frac{1}{2}\eta\ (^1E)$	$A\ (28, 1) = -\dfrac{3^{\frac{1}{2}}}{2.2^{\frac{1}{2}}}, A\ (28, 26) = \frac{1}{4}$

* The wavefunctions are labelled according to Table A24 of ref. 29 *i.e.* {term; m_s; orbital basis; (e^2 term component)}. Orbital symbolism: $\theta = d_{z^2}$, (ξ) $= d_{yz}$, $\eta = d_{xz}$.

Calculations. The calculations of the magnetic susceptibilities of the complexes exhibiting quartet interactions, [{Co(salen)}$_2$] and [Co(salen)]·py, required the diagonalization of a 28 × 28 matrix, while those which did not, [{Co(tsalen)}$_2$] and other (unpublished) cobalt(II) chelates, required an 18 × 18 matrix. Only those excited states from the $t_2^6e^1$ and $t_2^5e^2$ configurations which coupled directly by spin–orbit coupling to the ground state were included. The states derived from $^2T_2(^1A_1)$ were excluded as they are expected to be rather high in energy, and the influence on the magnetic behaviour is mimicked by the states derived from $^2T_2(^1E)$, although it must be borne in mind that the calculated energies for these latter states will be rather lower than is actually the case because of the neglect of $^2T_2(^1A_1)$. To further minimize parameter variation, the one-electron spin–orbit coupling constant, ζ, was set at 500 cm^{-1}, slightly reduced from the free-ion value. Any symmetry mixing of states was neglected. A summary is given below of the effect of the energies of the excited states on the calculated susceptibilities. It was quickly found that the ground state for all complexes was $^2E\theta$, *i.e.* the unpaired electron is in the d_{z^2} orbital. To first order, we have already shown the effect of the excited states on the g values for a d_{z^2} ground configuration.[28]

(a) $^2T_1$ *and* $^4T_1$ *States.* The spin-quartet states only affect the susceptibilities to second order *via* spin–orbit coupling. The $^4T_1(^3A_2)$ (x, y, z) states increase the first-order Zeeman term on approaching the ground state for all three directions. The $^4T_1(^3A_2)$ (x, y) states also increase the second-order Zeeman terms in the x and y directions, but the $^4T_1(^3A_2)$ z term reduces it in the z direction. The $^2T_1(^3A_2)$ (x, y, z) states decrease the first-order Zeeman terms on approaching the ground state, but increase the second-order terms, whilst the $^2T_1$ (^1E) (x, y, z) states increase both first- and second-order Zeeman terms when the energy separation from the ground state decreases. Thus the origin of a large high-frequency (or second-order Zeeman) susceptibility is easily explained; the $^2T_1$ terms have a small effect on the low-frequency susceptibility because of the opposite sign of mixing into the ground state, but have an additive effect on the second-order Zeeman term.

(b) $^2T_2$ *States.* The $^2T_2(^1E)$ and $^2T_2(^1A_1)$ states behave in the same way, mixing into the ground state, and raising the susceptibilities in the x and y directions [$^2T_2$ (ξ) and $^2T_2$ (η) respectively] for both first- and second-order Zeeman terms.

Comparison of theory and observed data. We have already mentioned briefly the rapid increase in moment at higher temperatures for [{Co(salen)}$_2$] and [Co(salen)]·py, which suggests the possible importance of quartet-state interactions in these two complexes. The low-temperature region of the susceptibility plots (80—240 K) for these complexes and the whole of the temperature range for [{Co(tsalen)}$_2$] showed Curie–Weiss behaviour. These linear regions could be well fitted to the theoretical model described above, without the need of including quartet-state interactions in the case of [{Co(tsalen)}$_2$]. The substantial temperature variation in this Curie–Weiss region arises from a large second-order Zeeman term. The best-fit parameter values are given in Table 3, and a discussion of these is given below. The model was not, however, able to predict the rapid increase in μ at higher temperatures for the salen complexes.

A number of approaches were examined to try to explain the behaviour in this region. Mixing by spin–orbit coupling of the doublet ground state with excited spin-quartet states or a thermal population of these states could not reproduce the observed behaviour.[30,31]

---

[30] C. G. Barraclough, *Trans. Faraday Soc.*, 1966, 1033.

[31] C. M. Harris, T. N. Lockyer, R. L. Martin, H. R. H. Patil, E. Sinn, and I. M. Stewart, *Austral. J. Chem.*, 1969, **22**, 2105.

The existence together of doublet and quartet-state molecules, with a thermodynamic equilibrium between the two, was rejected both because of the lack of any direct structural evidence and the large number of rather *ad hoc* assumptions inherent in the model. The existence of such spin isomers is reasonably well established in some tris(monothioacetylacetonato)iron(III) chelates [32] and have been postulated to explain the anomalous behaviour of some terpyridylcobalt(II) [33] and tris(dithiocarbamato)iron(III) complexes,[34] although recent low-temperature *X*-ray studies cast doubts on the applicability of the method to the dithiocarbamate derivatives.[35] We prefer the present quantum-mechanical approach based on the electronic configuration of a single species and find that the only way to satisfactorily reproduce the higher-temperature data for [{Co(salen)}$_2$] and [Co(salen)]·py is to assume that small changes in the ligand field occur as the temperature varies. This is perhaps not surprising when excited quartet states are so close to the ground state. Furthermore, it has been shown that slight movement of the cobalt(II) ion out of the ligand plane tends to stabilize quartet states energetically,[36] *e.g.* [Co(msalen)]·H$_2$O * is high spin and the cobalt(II) ion is 0.2 Å further out of the plane [37] than in [{Co(salen)}$_2$] and [Co(salen)]·py (each 0.2 Å out of plane).[21–23] The changes in the ligand field were assumed not to significantly affect the molecular orientations and hence not the direction cosines in Table 2. The assumption of changes in ligand-field parameters with temperature has also been recently invoked in the case of some iron(III) octaethylporphyrin derivatives [38] and in earlier e.s.r. studies of some magnetically anomalous cobalt chelates.[39]

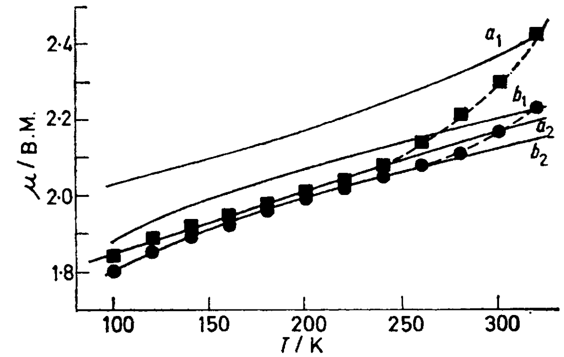

Figure 2 Effect on μ_f of varying the crystal-field parameters with temperature. Solid lines are calculated values for the best-fit parameters a_1 at 320 K and a_2 at $\leqslant$200 K for [Co(salen)]·py, and b_1 at 320 K and b_2 at $\leqslant$240 K for [{Co(salen)}$_2$] (see Table 3). Broken lines are the experimental curves for [Co(salen)]·py (■) and [{Co(salen)}$_2$] (●)

It follows from the above discussion that a single set of best-fit parameters was obtained for [{Co(tsalen)}$_2$] and for the Curie–Weiss regions of [{Co(salen)}$_2$] and [Co(salen)]·py. For the last complexes some of the ligand-field energy parameters were then varied as a function of temperature at higher temperature (Table 3). The effect of this is shown in Figure 2. The values of energies of the excited states deduced for best-fit should not be taken too literally, since small changes in one parameter can often be absorbed by changes in another parameter, and the value of ζ, the spin–orbit coupling constant, was fixed arbitrarily (at a reasonable value). However, the deduced energy parameters are in a physically reasonable range, and their variation is restricted considerably by the necessity of calculating all three principal susceptibilities with one set of parameters. Unfortunately it would be extremely difficult to obtain polarized spectral data for these complexes to confirm the positions and assignments of the excited states. The solution and solid-reflectance optical data which have been reported show considerable inconsistencies, although the general spread of transition energies lies within the values estimated here.[11–13,40] In the case of [{Co(salen)}$_2$], an antiferromagnetic exchange constant, J, of -40 cm^{-1} was included in the calculations, and experimental confirmation of this value was obtained from observation of the Néel temperature at *ca.* 46 K. A similar value of J was also incorporated into the [{Co(tsalen)}$_2$] calculations, no direct observation of T_0 being available in this case. It should be stressed that the curvature in K at high temperatures for [{Co(salen)}$_2$] and [Co(salen)]·py is not due to magnetic exchange, since J is zero in the pyridine adduct.

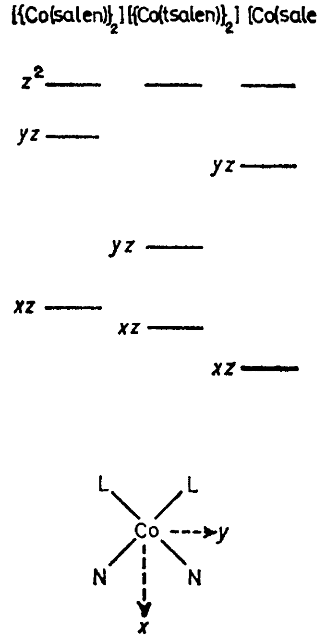

Figure 3 Ordering of out-of-plane d-orbital levels (not to scale)

DISCUSSION

In Figure 3 we show the relative ordering of the d-orbital levels, deduced from the energies of the excited

---

* msalen = NN'-Ethylenebis(3-methoxysalicylideneiminato).

[32] M. Cox and J. Darken, *Co-ordination Chem. Rev.*, 1971, **7**, 29.

[33] R. C. Stoufer, D. W. Smith, E. A. Clevenger, and T. E. Morris, *Inorg. Chem.*, 1966, **5**, 1167.

[34] R. L. Martin and A. H. White, *Transition Metal Chem.*, 1968, **4**, 114.

[35] J. G. Leipoldt and P. Coppens, *Inorg. Chem.*, 1973, **12**, 2269.

[36] J. A. Varga and C. A. L. Becker, *Canad. J. Chem.*, 1974, **52**, 79.

[37] M. Calligaris, G. Nardin, and L. Randaccio, *J.C.S. Dalton*, 1974, 1903.

[38] A. K. Gregson, H. A. O. Hill, and P. Skyte, personal communication.

[39] J. G. Schmidt, W. S. Brey, and R. C. Stoufer, *Inorg. Chem.*, 1967, **6**, 268.

[40] F. L. Urbach, R. D. Bereman, J. A. Topich, M. Hariharan, and B. J. Kalbacher, *J. Amer. Chem. Soc.*, 1974, **96**, 5063.

states. The anisotropy in the susceptibility of these molecules is dominated by the close approach of the d_{yz} orbital to the d_{z^2} ground-state orbital. The complex $[\{Co(tsalen)\}_2]$ is only weakly anisotropic because of the rather strong ligand field exerted by the sulphur atoms, which causes large orbital separations. The d_{yz} orbital consequently lies at a much lower energy in this case relative to that in $[\{Co(salen)\}_2]$ and $[Co(salen)]\cdot py$, the relative ordering of orbitals being the same for all three complexes.

It is pertinent to see if there is any relation between the electronic properties deduced here and the bonding of this type of cobalt(II) chelate to molecules such as pyridine and O_2. Pyridine is a weak σ donor ($k_b = 1.7 \times 10^{-9}$) and hence will only react to any significant extent with the cobalt complex if the latter is a sufficiently strong Lewis acid or, if this is not the case, if there is a significant π bonding to ensure the stability of the resulting complex. Both σ and π bonding will generally therefore be present in such a cobalt–pyridine linkage. The complex $[\{Co(salen)\}_2]$ reacts readily with pyridine to form stable $[Co(salen)]\cdot py$. The latter reacts further, to some extent, with pyridine. The complex $[\{Co(tsalen)\}_2]$ reacts only weakly with pyridine.[19,41] *X*-Ray structures on five-co-ordinate pyridine [6,24,42–44] or phenyl [45] derivatives of these chelates show that the axial group invariably lies almost exactly in the *yz* plane. Because of the steric constraints imposed by the ethylene bridge of the chelate back bonding though π orbitals on the metal will play an important rôle only if the orbitals are suitably oriented. The appropriate orbital in this situation is the out-of-plane d_{xz} orbital, which must of course have a favourable energy. The present results correlate well with this line of argument, the d_{xz} orbital in $[\{Co(salen)\}_2]$ being of suitable energy relative to pyridine p_π orbitals for strong bonding, whilst that of $[\{Co(tsalen)\}_2]$, at much lower energy, will lead only to weak bonding. The argument is further substantiated in the case of [Co(5Cl-amben)],* a related complex which does not react with pyridine; the d_{xz} and d_{yz} orbitals are in reverse order relative to the present situation.[16,28]

The bonding of O_2 to form 1 : 1 adducts of the type $[CoL(py)]\cdot O_2$ (L = chelate ligand) can be rationalized in a related manner. The O_2 molecule has the bent configuration and lies in the *xz* plane perpendicular to the axial base which is in the *yz* plane.[6,43] This suggests that the out-of-plane d_{yz} orbital on cobalt may be involved to some extent in π bonding to the oxygen molecule, there being no steric restraints imposed by the chelate ligand. π Bonding to d_{yz} is necessitated by the prior involvement of d_{xz} with the axial base. In a recent bonding scheme deduced for such complexes (L = porphyrin), the π bonding between Co and O_2 was considered to be reduced relative to σ bonding, because of the bent nature of the Co–O–O moiety.[46]

The inactivity of cobalt(II) complexes of the present type towards oxygen in the solid state would appear to be chiefly a function of the crystal packing, since e.s.r. data on active solutions of [Co(salen)] in pyridine suggest that the electronic structure is very similar to that deduced here for the solid. It would be most useful to have the *X*-ray structure and crystal anisotropy of the active solid form.

We thank the Australian Research Grants Committee for support, Professor B. O. West for advice and encouragement, Mr. A. van den Bergen and Mr. M. F. Corrigan for experimental assistance, and Drs. A. K. Gregson and J. E. Davies for help with computer programs.

[5/1484 *Received, 28th July*, 1975]

---

* 5Cl-amben = *NN'*-ethylene(bis-2-amino-5-chlorobenzylideneiminato).

[41] M. F. Corrigan, unpublished work.

[42] M. Calligaris, G. Nardin, and L. Randaccio, *Inorg. Nuclear Chem. Letters*, 1972, **8**, 477.

[43] M. Calligaris, G. Nardin, L. Randaccio, and G. Tauzher, *Inorg. Nuclear Chem. Letters*, 1973, **9**, 419.

[44] M. Cesari, G. Neri, G. Perego, E. Perrotti, and A. Zazzetta, *Chem. Comm.*, 1970, 276.

[45] S. Brückner, M. Calligaris, G. Nardin, and L. Randaccio, *Chem. Comm.*, 1970, 152.

[46] B. B. Wayland, J. V. Minkiewicz, and M. E. Abd-Elmageed, *J. Amer. Chem. Soc.*, 1974, **96**, 2795.